Hittite Journal of Science and Engineering, 2018, 5 (1) 49-55
ISSN NUMBER: 2148-4171
DOI: 10.17350/HJSE19030000077

Synthesis, characterization and electrochemical performance of Nb doped $LiFePO_4$/C cathodes

Cengiz Bağcı and Öncü Akyıldız
Hitit University, Department of Metallurgical and Materials Engineering, Corum, TURKEY.

ABSTRACT

We synthesized Nb-doped $LiFePO_4$/C nano composite cathode materials by mechanochemical activation followed by a single step calcination. The starting chemicals of Li_2CO_3, $FeC_2O_4.2H2O$, $NH_4H_2.PO_4$ and $C_6H_8O_7$ as lithium, iron, phosphate, and carbon sources are mixed in a high energy ball mill (250 rpm, 5h) and calcined at 650 °C and 10 hours. The resultant materials are structurally (XRD, SEM, TEM) and electrochemically characterized and high purity $LiFePO_4$ with high electrochemical performance is obtained. Voltage vs. specific capacity, discharge capacity vs. cycle number in manufactured battery is presented. An initial specific discharge capacity of 153 $mAhg^{-1}$ and a specific discharge capacity of 128.4 $mAhg^{-1}$ after the 8th charge/discharge cycling at 1C is recorded.

Keywords:
$LiFePO_4$, Lithium ion battery, Mechanochemical activation, Nb doping

Article History:
Received: 2017/08/14
Accepted: 2017/10/11
Online: 2018/03/28

***Correspondence to**: Cengiz Bağcı*
Department of Metallurgical and Materials Engineering, Hitit University, 19030, Corum, Turkey.
E-Mail: cengizbagci@hitit.edu.tr

INTRODUCTION

Rechargeable lithium-ion battery with lithium iron phosphate ($LiFePO_4$, LFP) cathode has found worldwide use in the consumer electronics, hybrid and electric automotive sectors due to its long cycle life, thermal stability, and high reliability. Cathodes consisting of LFP particles can achieve high charge/discharge rates and capacity, only if a conductive carbon mesh covers the surface of the particles to provide electronic conduction between the particles and if the distance between the particles is reduced to decrease the diffusion path. Accordingly, it has been shown that composite cathode batteries consisting of carbon coated nano-sized LFP particles can reach high charge / discharge rates and capacities [1]. Moreover, doping of metal ions (such as ions of Nb, V, Mg, etc.) are also used to distort the olivine lattice of LFP and result in an increased Li-ion transport and conductivity [2].

There are several solid-state and solution-based production methods available for the production of this cathode material, yet one of the most frequently used method is the mechanochemical activation [3]. The method is based on the principle of increasing the chemical reactivity of the mixture in a high-energy ball milling through attritors. By this method powders with low particle size and high surface area can be prepared. Similarly, LFP powders prepared by mechonochemical activation reported to have high purity, uniform and well-crystallized structure and exhibit high specific capacity as detailed in the following paragraph.

Franger et al. [4] observed formation of well crystallized, phase pure homogeneous $LiFePO_4$/C particles after adding sucrose to iron (II) phosphate ($Fe_3(PO_4)_2.5H_2O$), tri-lithium phosphate (Li_3PO_4) starting materials, milling 24 hours in planetary ball mill and calcining them at 550 ° C for 15 minutes under nitrogen atmosphere. Crystallization occurred at low temperature (432 ° C) due to deep grinding. In another work, Franger et al. [5] produced same material using saccharose and boron phosphate (BPO_4) for enhancing electronic conductivity and reported an improved electrochemical performance. Park et al. [6] observe that wet-mechanochemical activation in acetone provides approximately 74% capacity increase over dry grinding. Shin et al. [7] characterized carbon coated and chromium doped $LiFePO_4$ materials synthesized by mechanochemical activation and calcination of lithium carbonate (Li_2CO_3), iron oxalate dihydrate

($FeC_2O_4.2H_2O$) and ammonium dihydrogen phosphate ($(NH_4)_2.PO_4$) starting materials. Compared to bare $LiFePO_4$, carbon coated $LiFePO_4$ showed a significant increase in the rate performance, while the highest enhancement was achieved in Cr doped and carbon coated $LiFePO_4$. Li et al. [8] investigated the electrochemical properties of $LiFe_{1-x}Mn_xPO_4/C$ (glucose as carbon source) composite material produced by Mn addition during mechonochemical activation. It is observed that Mn doping improve electrochemical performance especially at high charge/discharge rates. Park et al. [9] investigated the main causes of the increase in the charge/discharge rate with the Al^{3+}, Cr^{3+} ve Zr^{4+} cation doping on the LFP samples produced by a single calcination step after mechanochemical activation. To this end, the bonding energies of $LiFePO_4/C$ and $LiFe_{0.97}M_{0.03}PO_4/C$ ($M=Al^{3+}$, Cr^{3+}, Zr^{4+}) materials were measured by XPS. The weakening of the Li-O bond and the facilitation of lithium diffusion have been reported as the main cause of the increase in rate performance with metal addition. Similarly, Ma et al. [10], Zhou et al. [11], and Zhao et al. [12] have prepared Nb doped $LiFePO_4/C$ powders with improved electrochemical activity.

The mechanochemical method is also used as a second process to reduce the particle size or to obtain a composite powder for powders previously produced by other methods. For example, Morales et al. [13] compared the performance $LiFePO_4$ particles after applying mechanochemical activation. Some of the most commonly used starting materials in the literature for the production of $LiFePO_4$ by mechanochemical activation are lithium carbonate (Li_2CO_3), iron oxalate dihydrate ($FeC_2O_4.2H_2O$) and ammonium dihydrogen phosphate. Table 1 provides a list of references that have been compiled for mechanochemical activation of these materials.

In Table 1, parametric studies carried out on the amounts of carbon and additive metal, ball to powder ratio or calcination temperature is listed. Table 2 gives the

Table 1. A list of elements used in lithium, iron, phosphate, carbon sources and doping elements used for LFP - LFP/C synthesis by mechanochemical activation method. Thermal and structural analysis methods can be read from the relevant columns.

#	Source of			C*	Dopant	Thermal analysis*	Structural analysis*	Reference
	Li	Fe	PO_4					
1				CB	Cr^{3+}	-	isXRD,SEM	[7]
2				-	-	-	XRD,HRTEM	[6]
3				CB	Cr^{3+}, Al^{3+}, Zr^{4+}	-	XRD,SEM	[9]
4				-	Nb^{5+}	-	ABF-STEM	[14]
5				CA	-	TG/DSC	XRD,FTIR,SEM	[15]
6				-	-	-	XRD	[16]
7	Li_2CO_3			AC	-	-	XRD,SEM,TEM	[17]
8		$FeC_2O_4 \bullet 2H_2O$	$NH_4H_2PO_4$	-	-	-	XRD,SEM	[18]
9				-	-	-	XRD	[19]
10				-	-	TG	XRD,FE-SEM	[20]
11				-	-	TG/DTG	XRD,EDS,SEM,TEM	[21]
12				MA	-	DSC	XRD,SEM,TEM,EDS	[22]
13				MA	-	-	XRD,SEM,TEM/EDS	[23]
14				PVA	-	TG	XRD,SEM	[24]
15	LiF			-	-	TG/DSC	XRD,SEM	[25]
16	$Li(OH)H_2O$			-	-	-	-	[8]
17		$FePO_4 \bullet 2H_2O$		CS	-	-	XRD,SEM,TEM	[26]
18	Li_2CO_3			SC		TGA	isXRD	[27]
19	Li_3PO_4	$Fe_3(PO_4)_2 \bullet 5H_2O$		SC	-	TGA/DSC	XRD,SEM	[4]
20					-	-		[5]
21	LiH_2PO_4	Fe_2O_3	LiH_2PO_4	CA	Nb^{5+}	NA	XRD,FE-SEM	[27]

*

CA: Citric acid
CB: Carbon black
SC: Saccharose
TA: Tartaric acid
PEG: Polyethylene glycol
AC: Acetylene black
CS: Cane sugar
MA: Malic acid

TGA: Termogravimetric analysis
DTA: Differential thermal analysis
DSC: Differential scanning calorimetry
isXRD: in situ X-ray diffraction
SEM: Scanning electron microscopy
HRTEM: High resolution transmission electron microscopy
EDS: Energy dispersive spectroscopy
FE-SEM: Field emission SEM

D: Doping
C: Carbon
T: Temperature
mt: Milling time
BP: Ball/powder ratio
w: Wet milling
RT: Room temperature
atm: Atmosphere

Table 2. Details of carbon and metal doping type and amount, calcination and mechano-chemical activation methods used in the studies given in Table 1.

#	C (w %)	Dopant	Calcination			Activation				
			°C	hr	atm	b:p	hr	°C	rpm	atm
1	3	Cr^{3+}, 0.02	600/750	10	Ar+%5 H_2	20:1	3	RT	250	
2	-	-	600	10	Ar+%5 H_2	20:1	3	RT	250	
3	3	Cr^{3+},Al^{3+},Zr^{4+}	750	10	Ar+%5 H_2	20:1	3	RT	250	
4	-	Nb^{5+}, 0.02	800	10	Ar					
5	0/5/6/6.75/8	-	700	20	N_2, dyn	10:3	2	RT	400	Ar
6	-	-	700	10	Vakum		1			
7	7.8/4.7	-	600	10	N_2	10:3	15	RT	1000	Ar
8	-	-	600+700	0.5	N_2		2			
9	-	-	400/600	2/4	Ar	20:1/40:1	0.5		660	
10	-	-	50+350+650	16+4+10	Ar+%5 H_2		24			
11	-	-	350+600+800	8+8	Ar	1:20	2			
12	50	-	873	12	Ar+%5 H_2	1:20	3/12/18		300	
13	60	-	60+320+600	10+12	Ar+%5 H_2		3			
14	0/1/3/5/10/30	-	800/300+800/500+800	9/6+9	Ar		24			
15	-	-	300/400/500/600/700/800	8/24	Ar+%8 H_2					
16		-								
17	20	-	60+650	8.5	N_2	15/20/25/30:1	2.5		3000	
18	-	-	500+120+600	6+5	Ar		2		450	
19	-	-	550	0.25	N_2		24			
20	-	-	700		N_2					
21	5	Nb^{5+},0.005/0.01/0.015/0.025	700	12/4	N_2		5/6			

details of carbon and metal doping sources and amounts, calcination and mechanochemical activation methods for the studies given in Table 1.

In light of the literature review presented above, the aim of this work is to produce $LiFePO_4$/C nano composite cathode material with high purity and high electrochemical performance using the mechanochemical activation method by selected process parameters from Table 1 and 2.

MATERIALS AND METHODS

Lithium carbonate (Li2CO3, Abcr, Germany), iron oxalate dihydrate (FeC2O4.2H2O, Alfa Aesar, USA) and ammonium dihydrogen phosphate (NH4H2.PO4, Merck, Germany) were used as lithium, iron and phosphate sources respectively. Citric acid (C6H8O7, Merck, Germany) was used as a carbon source and niobium pentaoxide (Nb2O5, Sigma Aldrich, USA) as a niobium source. These precursor materials were mixed in stoichiometric

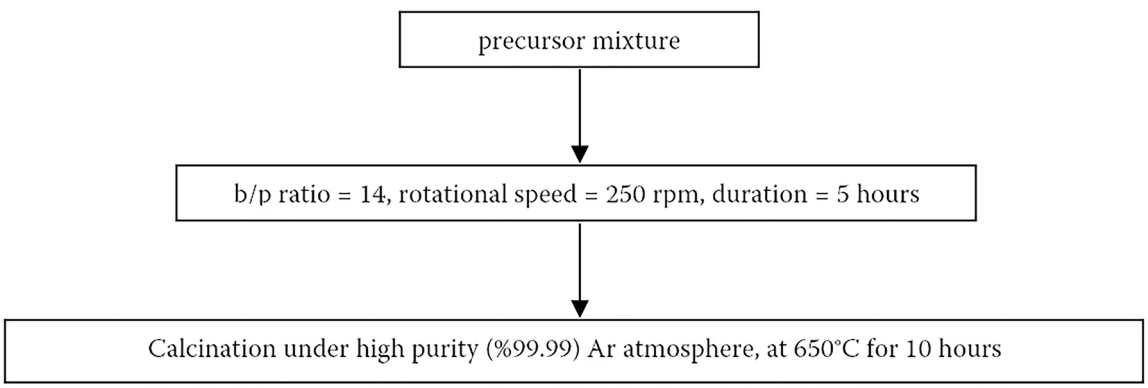

Figure 1. Flowchart of the synthesis method.

amounts for 2.4 at. % Nb and at. 6.4% carbon and then ball-milled for 5 h in a planetary mill using zirconium dioxide vessel and balls (diameter 10mm) with a ball to powder ratio of 14.0. The resulting mixture was calcined in a tubular furnace (Protherm PTF 16/75/450) under argon flow at 650 °C for 10 h in order to obtain the Nb-doped LiFePO4/C composite powders. Flowchart for the synthesis method is presented in Fig. 1.

XRD analysis was performed using a Bruker D8 Advance diffractometer equipped with a Cu Kα source (λ = 0.15406 nm). Tests were carried out at 40 kV, 30 mA, and the Bragg angle (2θ) varied from 5° to 80° with a scan rate of 1°/min. Powder morphologies were investigated using a SEM (FEI / Quanta 450 FEG) and TEM (FEI-TECNAI).

Cast electrodes were prepared from a 500 mg mixture of 85 wt % of LFP/C active material, 10 wt % of carbon black (Abcr, Germany) conductive additive and 5 wt % of PVDF (polytetrafluoroethylene, (Sigma Aldrich, USA) binder was mixed in N-methylpyrrolidone (NMP, Merck, Germany) for 1.5 hours to obtain a thick slurry. This slurry was then cast on an aluminum foil with a blade spacing of 100 µm and dried in an oven at 100° C for 12 hours. Discs of 9.525 mm in diameter punched from these films in glove box (Inert I-Lab 2GB) were used as cathode. For anode, discs were cut from a metallic lithium rod (Alfa Aesar, USA) with a diameter of 12.7 mm. 1M $LiPF_6$ (lithium hexafluorophosphate, Abcr, Germany) solution in 1:1 ethylene carbonate ($C_3H_4O_3$, Abcr, Germany): dimethyl carbonate ($C_5H_{10}O_3$, Abcr, Germany) was prepared as the liquid electrolyte.

Cathode and anode discs, bottom and top covers of CR2032 button battery cell, spring and spacers and electrolyte-impregnated (16 mm in diameter) glass fiber filter paper separator (691 VMR, France) were assembled using an electric coin cell crimping machine (MTI – MSK-160D) inside the glovebox. The electrochemical measurements were conducted with a custom designed

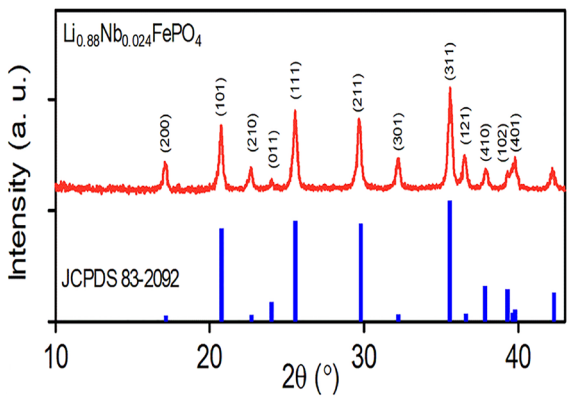

Figure 2. XRD pattern of 2.4% Nb-doped $LiFePO_4$/C powders.

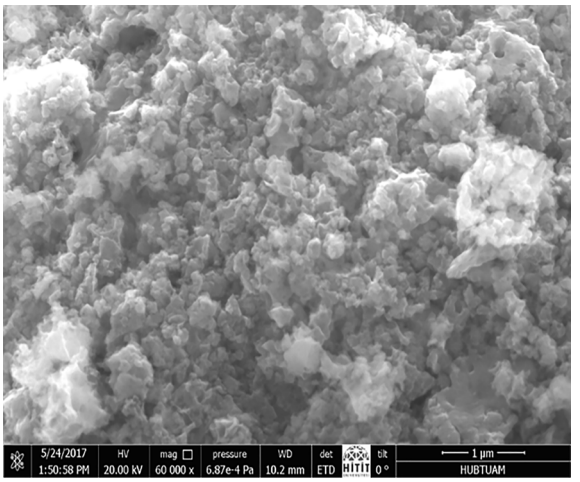

Figure 3. SEM image of 2.4% Nb-doped LiFePO4/C powders.

(max. 30mV) battery tester (UBA 5, Vencon Technologies, Canada).

In order to determine the specific capacity of the cell, weight of the electrode disc with the current collector (W_{ED}), weight of the uncoated current collector disc of the same diameter (W_{CC}) were measured and weight of electrode material were calculated by taking their difference. Then the weight of active material in the electrode is calculated by: W_{AM} = 85 % (W_{ED} - W_{CC}). Multiplying this value with the theoretical specific capacity of LFP (C = 170 $mAhg^{-1}$) the theoretical specific capacity of the electrode disc (C_{ED}) is obtained: C_{ED} = C x W_{AM} [28]. Then the coin cell was first charged under a constant voltage of 3.6V, rested for five minutes and discharged at constant current at 1C (discharge in 1 hour). This charge and discharge cycle has been repeated eight times.

RESULTS AND DISCUSSION

Fig. 2 shows the XRD pattern of 2.4 at. % Nb-doped $LiFePO_4$/C powders. The crystal phase is ordered olivine structure indexed orthorhombic Pnma, and no other impurity peak is detected. Comparing the $Li_{1-5x}Nb_xFePO_4$ (x=0.024) pattern with that of JCPDS card number 83-2092, one can conclude that doping this amount of Nb do not affect the structure of the sample. Yet considering the ionic radii of Nb5+ (78 pm) is larger than that of Li+ (68 pm), the enlarged crystal cell volume with Nb ion doping is expected to improve the lithium ion diffusivity [27] and in turn electrochemical performance.

The crystallite diameter (d) was calculated from the XRD line width using the Scherrer equation, $d = 0.9\lambda/(\beta_{1/2}\cos\theta)$, where λ is the X-ray wavelength, $\beta_{1/2}$ is the calculated width at half-maximum of the diffraction peak, and θ is the diffraction angle. Value of d is measured at the angle corresponding to the (311) line and found as 52 nm.

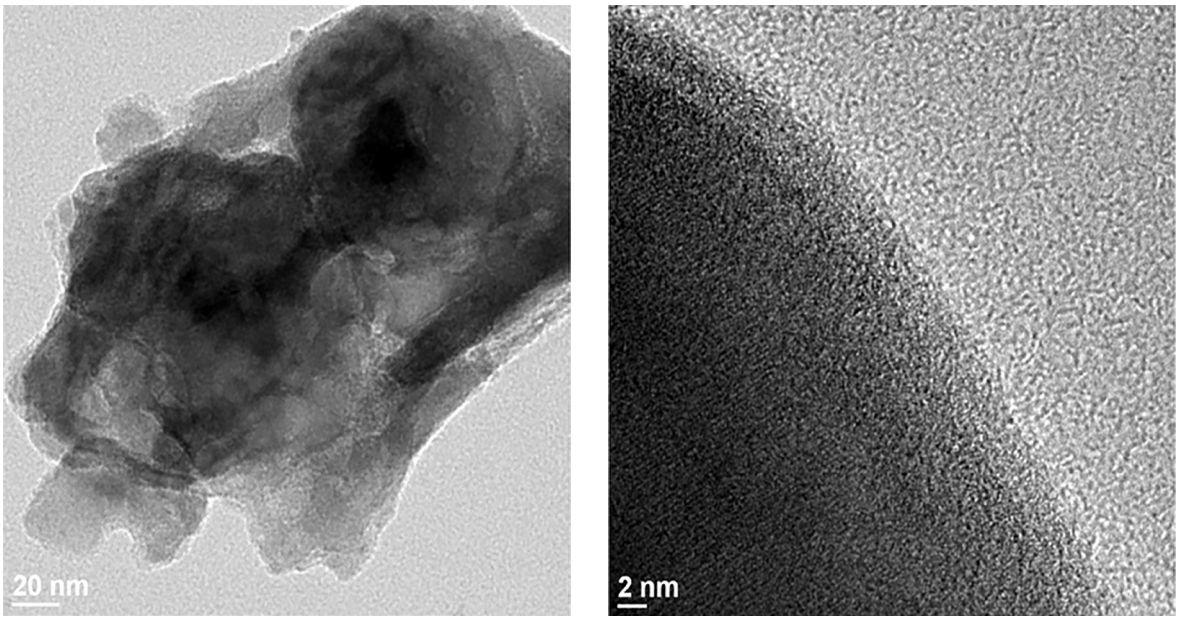

Figure 4. TEM images of 2.4% Nb-doped LiFePO4/C powders.

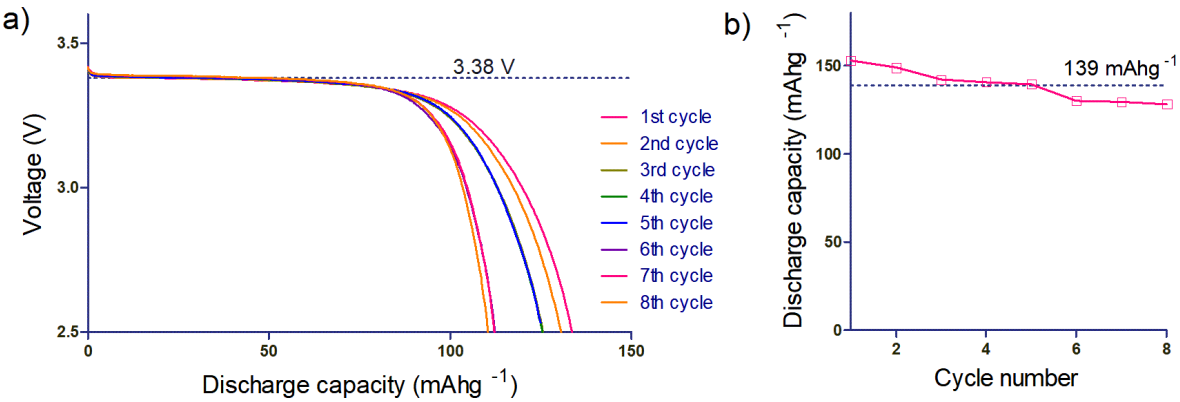

Figure 5. a) Discharge curves and b) cycle life performance of CR2032 button battery cell with a positive electrode prepared from 2.4 at. % Nb-doped $LiFePO_4$/C powders operated between 3.5 and 2.5 V at the current rate of 1 C.

Fig. 3 shows the scanning electron microscopy (SEM) image of 2.4 at. % Nb-doped $LiFePO_4$/C powders, where powders are consisting of agglomerated particles.

Fig. 4 shows the TEM images of 2.4 at. % Nb-doped $LiFePO_4$/C powders where it seen that the particles are coated and connected by carbon. Fig. 4a confirms that the particles had a size of 50~100 nm with a circular and oval shape. The particle size reported here is in good aggrement with the calculated crystallite size (52 nm) using the Scherrer equation. From Fig. 4b, it is clear that the carbon coating is uniform, and the shell thickness of the coating is in the range of ~3 nm, indicating that carbon could inhibit the particle growth, and help in obtaining smaller particles [29].

Fig. 5a shows discharge curves of the CR2032 button battery cell with a positive electrode prepared from 2.4 at. % Nb-doped LiFePO4/C powders. The discharge capacity at the rate 1 C, was about 139 $mAhg^{-1}$ between a cutoff voltage of 2.5 and 3.5 V. Also, a good voltage plateau was observed at about 3.4 V (vs. Li/Li+). Fig. 5b shows the cycle performance at 1 C rate. An initial specific discharge capacity of 153 $mAhg^{-1}$ and a specific discharge capacity of 128.4 $mAhg^{-1}$ is recorded after the 8th charge/discharge cycling.

CONCLUSION

We synthesized Nb doped $LiFePO_4$/C nano composite cathode materials by mechanochemical activation at 250 rpm for 5 hours followed by a calcination at 650 °C for 10 hours. The resultant materials are structurally (XRD, SEM, TEM) and electrochemically characterized. LFP with high electrochemical performance is obtained. The discharge capacity at the rate 1 C, is about 139 $mAhg^{-1}$

and a good voltage plateau is observed at about 3.4 V (vs. Li/Li+). A specific discharge capacity of 128.4 $mAhg^{-1}$ is recorded after the 8th charge/discharge cycling at 1C.

ACKNOWLEDGEMENTS

This work was supported by the Hitit University Scientific Research Projects Funding Program through a research Grant No. MUH190001.15.02. The authors wish to thank Prof. I. Sonmez for his interest in this work and Res. Assts. B. Alkan and D. Candemir of Hitit University for their help with the laboratory instruments.

REFERENCES

1. Xie G, Zhu H–J, Liu X–M, and Yang H. A core-shell LiFePO4/C nanocomposite prepared via a sol-gel method assisted by citric acid. Journal of Alloys and Compounds 574 (2013) 155-160.
2. Johnson ID, Blagovidova E, Dingwall PA, Brett DJL, Shearing PR. Darr JA. High power Nb–doped LiFePO4 Li–ion battery cathodes; pilot–scale synthesis and electrochemical properties. Journal of Power Sources 326 (2016) 476e481
3. Toprakci O, Toprakci HAK, Ji L, Zhang X. Fabrication and electrochemical characteristics of $LiFePO_4$ powders for lithium–ion batteries. Kona Powder and Particle Journal 28 (2010) 50–72.
4. Franger S, Cras FL, Bourbon C, Rouault H. Comparison between different LiFePO4 synthesis routes and their influence on its physico–chemical properties. Journal of Power Sources 119-121 (1) (2003) 252-257.
5. Franger S, Benoit C, Bourbon C, Cras FL. Chemistry and electrochemistry of composite LiFePO4 materials for secondary lithium batteries. Journal of Physics and Chemistry of Solids. 67 (5–6) (2006) 1338-1342.
6. Park CK, Hwang JT, Cho WI and Jang H. The origin of the residual carbon in LiFePO4 synthesized by wet milling. Bull Korean Chem Soc. 32 (2) (2011) 536–540.
7. Shin HC, Park SB, Jang H, Chung KY, Cho WI, Kim CS, Cho BW. rate performance and structural change of cr–doped LiFePO4/C during cycling. Electrochemica Acta 53 (2008) 7946-7951.
8. Li C, Hua N, Wang C, Kang X. Effect of Mn^{2+} doping in LiFePO4 and the low temperature electrochemical performances. Journal of Alloys and Compounds 509 (2011) 1897-1900.
9. Park CK, Park SB, Park CH, Shin HC, Cho WI and Jang H. The root cause of the rate performance improvement after metal doping: a case study of LiFePO4. Bull Korean Chem Soc. 32 (3) (2011) 921–926.
10. Ma Z, Shao G, Wang G, Zhang Y and Du J. Effects of Nb–doped on the structure and electrochemical performance of $LiFePO_4$/C composites. Journal of Solid State Chemistry 210 (1) (2014) 232-237.
11. Zhang, Q, Wang S, Zhou Z, Ma G, Jiang W, Guo X, Zhao S. Structural and electrochemical properties of Nd–doped LiFePO4/C prepared without using inert gas. Solid State Ionics 191 (2011) 40-44.
12. Zhuang D, Zhao X, Xie J, Tu J, Zhu T, Cao G. One–step Solid–state Synthesis and Electrochemical Performance of Nb–doped LiFePO4/C. ActaPhys.Chim.Sin. 22 (2006) 840-844.
13. Morales J, Trócoli R, Rodríguez–Castellón E, Franger S, Santos–Peña J. Effect of C and Au additives produced by simple coaters on the surface and the electrochemical properties of nanosized LiFePO4. Journal of Electroanalytical Chemistry 63 (2009) 29-35.
14. Suo L, Han W, Lu X, Gu L, Hu YS, Li H, Chen D, Chen L, Tsukimoto S and Ikuhara Y. Highly ordered staging structural interface between $LiFePO_4$ and $FePO_4$. Phys Chem Chem. Phys. 14 (2012) 5363–5367.
15. Zhang D, Yu X, Wang Y, Cai R, Shao Z, Liao X–Z, and Ma Z–F. Ball milling–assisted synthesis and electrochemical performance of LiFePO4/C for lithium–ion battery adopting citric acid as carbon precursor. Journal of the Electrochemical Society 156 (10) (2009) A802– A808.
16. Li M, Xie K, Li D, and Pan Y. Synthesis of LiFePO4 by one–step annealing under the vacuum condition. Journal of Materials Science 40 (2005) 2639-2641.
17. Kim J–K, Choi J–W, Chauhan GS, Ahn J–H, Hwang G–C, Choi J–B and Ahn H–J. Enhancement of electrochemical performance of lithium iron phosphate by controlled sol–gel synthesis. Electrochimica Acta 53 (28) (2008) 8258-8264.
18. Koltypin M, Aurbach D, Nazar L and Ellis B. More on the performance of $LiFePO_4$ electrodes–the effect of synthesis route, solution composition, aging, and temperature. Journal of Power Sources 174 (2) (2007) 1241-1250.
19. Kosova N, Devyatkina E. On mechanochemical preparation of materials with enhanced characteristics for lithium batteries. Solid State Ionics 172 (1–4) (2004) 181-184.
20. Lee J, Kumar P, Lee G, Moudgil BM and Singh RK. Electrochemical performance of surfactant–processed $LiFePO_4$ as a cathode material for lithium–ion rechargeable batteries. Ionics, 19(2) (2012) 371-378.
21. Ojczyk W, Marzec J, Świerczek K, Zając W, Molenda M, Dziembaj R and Molenda J. Studies of selected synthesis procedures of the conducting LiFePO4–based composite cathode materials for li–ion batteries. Journal of Power Sources 173(2) (2007) 700-706.
22. Fey GTK, Chen YG and Kao HM. Electrochemical properties of $LiFePO_4$ prepared via ball–milling. Journal of Power Sources 189 (1) (2009) 169-178.
23. Fey GTK and Lu TL. Morphological characterization of $LiFePO_4$/C composite cathode materials synthesized via a carboxylic acid route. Journal of Power Sources 178 (2) (2008) 807-814.
24. Yun NJ, Ha HW, Jeong KH, Park HY and Kim K. Synthesis and electrochemical properties of olivine–type $LiFePO_4$/C composite cathode material prepared from a poly(vinyl alcohol)–containing precursor. Journal of Power Sources 160 (2) (2006) 1361-1368.
25. Wang D, Li H, Wang Z, Wu X, Sun Y, Huang X and Chen L. New solid state synthesis routine and mechanism for $LiFePO_4$ using LiF as lithium precursor. Journal of Solid State Chemistry, 177(12) (2004) 4582-4587.
26. Lv YJ, Su J, Long YF, Cui XR, Lv XY and Wen YX. Effects of ball–to–powder weight ratio on the performance of $LiFePO_4$/C prepared by wet–milling assisted carbothermal reduction. Powder Technology 253 (2014) 467-473.
27. Chen Z, Ren Y, Qin Y, Wu H, Ma S, Ren J, He X, Sun YK, Amine K. Solid state synthesis of $LiFePO_4$ studied by in situ high energy x–ray diffraction. Journal of Materials Chemistry 21(15) (2011) 5604-5609.

28. Kayyar A, Huang J, Samiee M, Luo J. Construction and testing of coin cells of lithium ion batteries. J Vis Exp 66 (e4104) (2012) 1-5.

29. Kim HS, Kam DV, Kim VS, Koo HJ. Synthesis of the $LiFePO_4$ by a solid-state reaction using organic acids as a reducing agent. Ionics 17 (4) (2011) 293-297.